N-Alkylcyanopyridinium-Mediated Photoinduced Charge Separation across Dihexadecyl Phosphate Vesicle Membranes

Sergei V. Lymar,[†] Rafail F. Khairutdinov,[‡] Valentina A. Soldatenkova, and James K. Hurst*

Department of Chemistry, Washington State University, Pullman, Washington 99164-4630

Received: November 6, 1997; In Final Form: February 10, 1998

The triplet-photoexcited [5,10,15,20-tetrakis(4-sulfonatophenyl)porphinato]zinc(II) (^{3}ZnTPPS^{4-}) ion underwent rapid one-electron oxidation by a series of *N*-alkyl-4-cyanopyridinium (C_nCP^+) ions. In aqueous solution, the quenching rate constants ($k_q \cong 4 \times 10^9$ M^{-1} s^{-1}) were insensitive to the *N*-alkyl chain length over the range examined ($n = 1-16$). Charge recombination was also rapid ($k_r \cong 1.3 \times 10^8$ M^{-1} s^{-1}) and independent of the chain length. However, when dihexadecyl phosphate vesicles were included in the reaction medium, both k_q and k_r decreased progressively with increasing chain length. The chain-length dependence of k_q was in quantitative accord with a dyamical model wherein the relative rate constants were determined by C_nCP^+ partitioning between the aqueous phase and the aqueous−organic membrane interface, with only the aqueous-phase component being reactive toward ^{3}ZnTPPS.$^{4-}$ The decrease in k_r with increasing chain length was attributed to capture of the neutral lipophilic C_nCP^0 radicals within the hydrocarbon phase of the membrane. Net photoinduced transmembrane reduction was observed in vectorially organized systems containing oxidants within the inner aqueous phase of the vesicles and sensitizer, C_nCP^+, and a sacrificial electron donor in the external aqueous phase. Transmembrane reduction of occluded Co(bpy)$_3^{3+}$ was accompanied by 1:1 stoichiometric uptake of C_nCP^+; the characteristic time for this step, determined by both transient kinetic spectroscopy and quantum-yield measurements under continuous photolysis, was 2×10^{-2} s, consistent with C_nCP^0 functioning as mobile transmembrane electron carriers. The overall quantum yield for photosensitized C_1CP^0-mediated transmembrane Co(bpy)$_3^{3+}$ reduction by dithiothreitol was $\phi \approx 0.7$. For long-chain analogues, ϕ was less, an effect that could be quantitatively accounted for by the corresponding decline in k_q values.

Introduction

Microphase-organized asymmetric redox systems have been extensively explored for application to solar photoconversion, molecular electronics, and biomimetics. One potentially fruitful approach to device fabrication utilizes closed bilayer membranes containing vectorially organized redox assemblies as simple analogues of the energy-transducing organelles of living cells.[1,2] In principle, the membrane can provide any of several critical functions,[3−5] including (1) dynamic control of individual reaction steps by interfacial adsorption of one or more of the reactants, (2) lifetime enhancement of reactive intermediary species by phase separation, and (3) energy transduction via membrane polarization that couples electrogenic transmembrane charge separation to other components capable of performing useful work.[6] The system design is dictated largely by the application envisioned. For example, membrane-based photocatalytic systems for water photolysis require high intercompartmental fluxes of redox intermediates, which (as discussed below) can only be achieved if the transmembrane redox pathways are electroneutral. In contrast, application as chemical analogues of electronic devices will almost certainly require membrane polarization, which can only be accomplished by transmembrane charge separation, that is, electrogenic redox pathways. Thus, a firm understanding of relationships among molecular structure, microphase topography, and chemical reactivity is prerequisite to successfully designing assemblies for specific tasks.

The most thoroughly studied artificial systems have utilized water-soluble porphyrins or ruthenium polyimines as photosensitizers and methyl viologen (*N*,*N*′-dimethyl-4,4′-bipyridinium, MV^{2+}) and its amphiphilic alkyl-substituted analogues as combined oxidative quenchers and transmembrane redox mediators. These components are vectorially organized around phospholipid liposomes or vesicles obtained from synthetic membrane-forming amphiphiles.[3−5,7−10] Mechanistic studies of these systems have provided considerable insight into the fundamental principles governing transmembrane oxidation−reduction. Specifically, we have shown[10,11] that net transmembrane oxidation−reduction mediated by methyl viologen can occur by either of two pathways, one involving transmembrane diffusion of the viologen radical cation (MV^+) and the other involving diffusion of the neutral species (MV^0) formed by disproportionation of MV^+; that is, $2MV^+ \rightarrow MV^{2+} + MV^0$. Transmembrane diffusion of MV^+ occurs without charge-compensating movement of other ions. Consequently, an electrical potential ($\Delta\psi$) develops that opposes further ion translocation. Translocation of the uncharged MV^0, however, does not contribute to membrane polarization, and its membrane permeability is not affected by the developing electrical potential arising from transmembrane diffusion of MV^+. The intrinsic permeability of MV^0 through dihexadecyl phosphate (DHP) unilamellar vesicle membranes is about 10^5-fold greater than that of MV^+ (when $\Delta\psi = 0$); the membrane is impermeable to

[†] Current Address: Department of Chemistry, Brookhaven National Laboratory, Upton, NY 11973.

[‡] Visiting Scientist from the N.N. Semenov Institute of Chemical Physics, Moscow 117334, Russia.

* To whom correspondence should be addressed. E-mail: hurst@wsu.edu. Fax: (509) 335-8867.

S1089-5647(98)00115-1 CCC: $15.00
Published on Web 03/20/1998

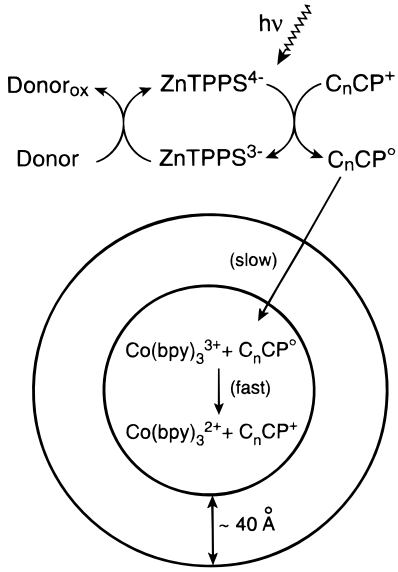

Figure 1. General reaction scheme for C_nCP^+-mediated photoinduced charge transfer.

MV^{2+} on the time scale of net transmembrane oxidation−reduction. Under the usual reaction conditions, the disproportionation equilibrium lies far to the left so that $[MV^+]/[MV^0] \simeq 10^5-10^6$. Thus, although its intrinsic permeability is markedly less, the net flux of MV^+ across the unpolarized DHP membrane is actually greater than that of MV^0. Translocation of only a few MV^+ ions across the bilayer gives rise to a substantial transmembrane potential, however, markedly retarding the diffusion rate of MV^+. Therefore, as the reaction proceeds, the major pathway changes from the electrogenic one with MV^+ as the electron carrier to the electroneutral one with MV^0 as the carrier.

Regardless of pathway, the net flux of the viologen-based electron carriers across the membrane is too low to be of practical utility. Transmembrane diffusion of MV^+ across DHP bilayers is inherently slow, that is, $k_t = 2.7 \times 10^{-2}$ s^{-1} at 23 °C, and although the corresponding diffusion rate constant for MV^0 is very high, that is, $k_t = 1.1 \times 10^3$ s^{-1}, the compound is present in only vanishingly small concentrations so that its net diffusion rate is also low.[11] To remedy this deficiency, we have sought to develop combined oxidative quenchers/electron carriers whose predominant one-electron-reduced states are uncharged and therefore capable of high rates of transmembrane diffusion. In the present study, a series of *N*-alkyl-4-cyanopyridinium ions have been prepared and their reactivities in DHP vesicle-organized photochemical systems containing compartmented [5,10,15,20-tetrakis(4-sulfonatophenyl)porphinato]zinc(II) ($ZnTPPS^{4-}$) ion and various electron donors and acceptors have been examined (Figure 1). In general, the reduction potentials of *N*-alkylpyridiniums are too low ($E° \leq -1$ V, NHE)[12] to function as oxidative quenchers of the $^3ZnTPPS^{4-}$ photoexcited ion; however, addition of strongly electron-withdrawing substituents such as the cyano group raise the potential to a level ($E° = -(0.5-0.65)$ V)[12-14] where electron transfer becomes thermodynamically favorable. Appending the cyano group at the ring 4-position also inhibits coupling of the reduced cyanopyridine radicals, minimizing degradative viologen formation.[15] We show herein that, as expected, *N*-alkyl-4-cyanopyridinium ions are highly efficient oxidative quenchers of $^3ZnTPPS^{4-}$ that are capable of rapidly transferring reducing equivalents across DHP membranes to occluded electron acceptors.

Experimental Section

Materials. 4-Cyanopyridine (Aldrich) was purified by recrystallization from ethanol. *N*-Methyl-4-cyanopyridinium iodide was prepared by refluxing 13 g (0.12 mol) of the cyanopyridine with 26 g (0.18 mol) iodomethane in 300 mL of ethanol for 6 h. The yellow-orange precipitate that had accumulated was isolated by filtration, washed with ether, air-dried, and recrystallized from ethanol. The absorption spectra of the radicals formed by photosensitized reduction (see below) of 36−250 μM of the salt in aqueous solution containing DHP vesicles, 1−12.5 μM $ZnTPPS^{4-}$, and either 15 mM triethanolamine (TEOA) or 210 μM dithiothreitol ($D(SH)_2$) were qualitatively identical to published spectra.[12] The molar extinction coefficient of the radical at its UV band maximum (298 nm) was determined by measuring the absorbance decrease following addition of deoxygenated solutions containing small known amounts of potassium ferricyanide to oxidize a fraction of the radical back to the cation. This one-electron oxidation occurred within the time of mixing and appeared as a step on the otherwise slow radical-decay profile arising from radical coupling to form methyl viologen.[15] From the magnitude of the spectral changes, a value of $\epsilon_{298} = 2.0 \times 10^4$ M^{-1} cm^{-1} was calculated. Other *N*-alkyl-4-cyanopyridinium salts were prepared by reacting 4-cyanopyridine with a 1:1 molar equivalent of the corresponding *n*-alkyl bromide in a sealed tube for 16−23 h at 70−95 °C; crude products were recrystallized from acetonitrile following addition of ether to induce precipitation. The recrystallized bromides gave single spots by thin-layer chromotography on silica (1/1 ethanol/formaldehyde); product identities were confirmed by NMR spectroscopy. Dihexadecyl phosphate was recrystallized from methanol after filtering to remove insoluble impurities. Concentrations of [5,10,15,20-tetrakis(4-sulfonatophenyl)porphinato]zinc(II) (Midcentury Chemicals) in reagent solutions were determined spectrophotometrically using $\epsilon_{421} = 6.8 \times 10^5$ M^{-1} cm^{-1}.[16] Tris(2,2′-bipyridyl)cobalt(III) perchlorate was prepared as described[17] and recrystallized from water. All other compounds were best-available grades that were used as received. Fresh stock solutions of $D(SH)_2$ were prepared prior to each set of experiments by dissolving weighed amounts of the free-flowing solid in buffer that had been deoxygenated by sparging with argon. All experiments were done in 20 mM Tris chloride, pH 8.0−8.3, which was prepared with water purified using a Milli-Q system.

Preparation and characterization of small unilamellar vesicles, including those containing $Co(bpy)_3^{3+}$ in their inner aqueous phase, are described in detail elsewhere.[10,18] Typical DHP concentrations in the vesicle suspensions were 4.5 mg/mL, which corresponds to a vesicle concentration of approximately 2 μM. The alkylpyridinium ions and $ZnTPPS^{4-}$ were subsequently added to the suspensions as required. Immediately prior to making photodynamic measurements, vesicle suspensions were deoxygenated by bubbling with purified Ar, after which portions of $D(SH)_2$ reagent solutions were added anaerobically using syringe-transfer techniques. The complete system (Figure 1) was highly photoreactive; consequently, suspensions containing $D(SH)_2$ were protected from photodegradation by working in a minimal red-light environment.

Continuous Photolyses. Continuous photolysis was performed using a 1.5 kW xenon lamp whose output was passed through aqueous $CuSO_4$ and appropriate light filters, then transferred via a flexible liquid light guide to the reaction cuvette, which was mounted in a Hewlet Packard 8452 diode array spectrophotometer interfaced to a ChemStation data

acquisition/analysis system. Light filters with cutoffs at 400 nm (or a 420 nm interference filter) and 515 nm were used for illumination in the zinc porphyrin Soret and Q-bands, respectively. Solutions were vigorously stirred during photolysis by means of a magnetic microbar contained within the sample cuvette. Reduction of $Co(bpy)_3^{3+}$ was monitored spectrophotometrically at 320 nm using $\Delta\epsilon_{320} = 2.85 \times 10^4$ M^{-1} cm^{-1} for the $Co(bpy)_3^{3+} - Co(bpy)_3^{2+}$ difference extinction coefficient.[10] Absolute quantum yields were determined at light intensities of $(2-8) \times 10^{-9}$ einstein/s as measured by potassium ferrioxalate[19] and Reinecke salt[20] actinometries or by a calibrated PowerMax 500D laser power meter thermoelectric bolometer. The quantum yield for ferrous ion formation in 0.15 M ferrioxalate[19] was taken to be 1.04 and, for photorelease of thiocyanate,[20] 0.31. The portion of energy absorbed by the photosensitizer was determined by comparing transmittances of solutions with and without added $ZnTPPS^{4-}$.

Transient-Kinetic Measurements. Absorption spectra and formation and decay kinetics of reaction intermediates were measured by laser flash photolysis using the second harmonic (532 nm) from a Continuum Surelite III Nd:YAG laser as the excitation source; pulse half widths were ~4 ns for outputs adjusted to 10−400 mJ/pulse. For uniformity of illumination, the light pulse was scattered by impinging it upon an unpolished wall of the spectral cell containing the sample, whose absorbance at 532 nm did not exceed 0.1. The analyzing beam, comprising filtered light from a 120 W mercury−xenon lamp configured in a crossed-beam arrangement to the exciting beam, was passed through the polished walls of the cuvette, dispersed with a McPherson model 272 monochromator, and light intensities at various wavelengths were recorded using a Hamamatsu R1477 photomultiplier assembly coupled to a Nicolet 4094/4184 digital oscilloscope. Both exciting and analyzing beams contained electronic shutters located between the light sources and sample that were synchronized with the laser pulse; this arrangement minimized light exposure of the sample during intervals when data were not being collected. The quantum yield for $^3ZnTPPS^{4-}$ formation was determined with this apparatus from ferrioxalate actinometry and the measured absorbance change at 460 nm assuming $\Delta\epsilon_{460} = 5.5 \times 10^4$ M^{-1} cm^{-1} for the $^3ZnTPPS^{4-} - ZnTPPS^{4-}$ difference extinction coefficient.[16] The value obatained, $\varphi = 0.86$, is nearly identical to the literature value[21] of $\varphi = 0.84$.

Reactant Distributions. The extent of binding of reactants to the DHP vesicles was determined using Centricon-10 centrifugal microconcentrators, whose membranes provided a 10 000 molecular-weight cutoff. In a typical experiment, 2.5 mL of a vesicle suspension containing $Co(bpy)_3^{3+}$, $ZnTPPS^{4-}$, or an *N*-alkyl-4-cyanopyridinium (C_nCP^+, where *n* refers to the number of carbon atoms in the *n*-alkyl chain) was centrifuged for 2.5 min at 4000 rpm using an SS-34 rotor in a Sorvall RC2-B centrifuge. Under these conditions, about 0.1 mL of solution containing low-molecular-weight species, including unbound reactant, passed through the membrane and was collected. Vesicle-bound reactants were retained, however, since the vesicles were too large to permeate the membrane. Because less than 5% of the solution volume was allowed to pass through the membrane, the concentration of reagents in the filtrate could be taken as equal to those of the unbound reagents in the vesicle suspension. The extent of binding was determined from the difference in concentrations of reactants in the filtrate and retentate, which were measured spectrophotometrically from their absorption maxima at 278 nm (C_nCP^+), 308 nm ($Co(bpy)_3^{3+}$), and 421 nm ($ZnTPPS^{4-}$). These measurements were corrected for nonspecific binding of ions by the microconcentrator membrane, which did not exceed 10% of the filtrate concentrations and for C_nCP^+ ions was independent of the alkyl chain length.

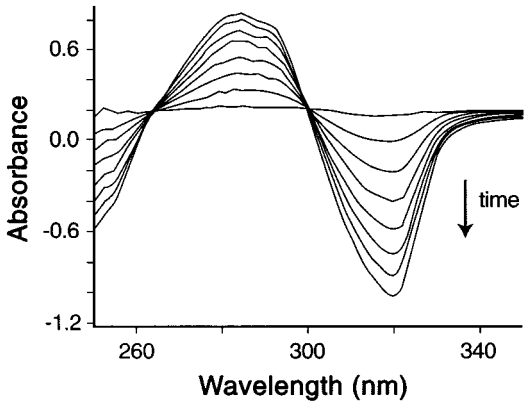

Figure 2. Difference absorption spectra accompanying illumination of the system shown in Figure 1. Trough-and-peak structure and isosbestic points are indicative of $Co(bpy)_3^{3+}$-to-$Co(bpy)_3^{2+}$ reduction.

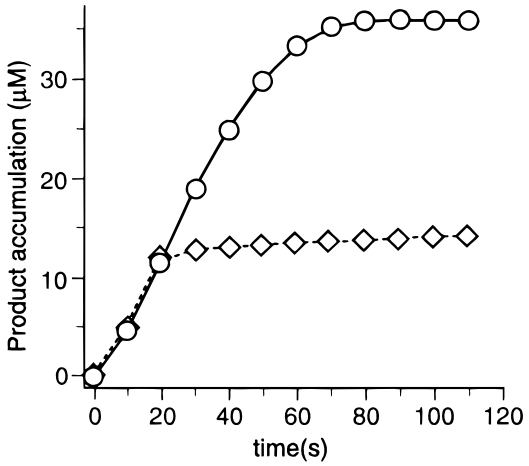

Figure 3. Kinetics of $Co(bpy)_3^{2+}$ accumulation monitored at 320 nm under continuous illumination of the $ZnTPPS^{4-}$ Q band: $[Co(bpy)_3^{3+}] = 33$ μM, $[ZnTPPS^{4-}] = 14$ μM, $[D(SH)_2] = 204$ μM, [DHP] = 8 mM, and $[C_1CP^+] = 100$ μM (◇) or 15 μM (○).

Results and Discussion

General Observations. All observations described in this section were qualitatively identical for photolysis in either Soret or Q bands of the porphyrin spectrum. Continuous illumination of the complete system (Figure 1) containing $Co(bpy)_3^{3+}$ in the internal aqueous phase and $ZnTPPS^{4-}$, C_1CP^+, and an electron donor ($D(SH)_2$ or TEOA) in the external aqueous phase gave rise to net reduction of the occluded $Co(bpy)_3^{3+}$ to $Co(bpy)_3^{2+}$ (Figure 2). The kinetics of $Co(bpy)_3^{3+}$ disappearance, monitored at 320 nm, are given in Figure 3 for two different reaction conditions. When $[C_1CP^+] > [Co(bpy)_3^{3+}]$, all of the internal oxidant could be reduced by photoexcitation of $ZnTPPS^{4-}$; however, when $[C_1CP^+] < [Co(bpy)_3^{3+}]$, only a fraction of the $Co(bpy)_3^{3+}$ corresponding to the initial C_1CP^+ concentration could be reduced. Similar data, taken over a wide range of experimental conditions, indicated that a 1:1 stoichiometric relationship exists between the extent of $Co(bpy)_3^{3+}$ reduction and the amount of C_1CP^+ added. Similar results were obtained when other C_nCP^+ ions were substituted for C_1CP^+, although for the long-chain analogues the rate of disappearance of $Co(bpy)_3^{3+}$ under continuous illumination was considerably de-

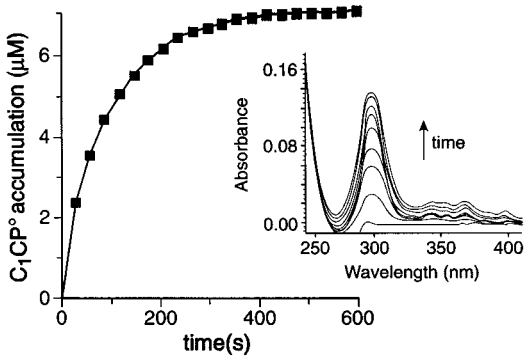

Figure 4. Kinetics of C_1CP^0 accumulation monitored at 300 nm under continuous illumination of the $ZnTPPS^{4-}$ Soret band with the intravesicular acceptor absent: $[ZnTPPS^{4-}] = 1\ \mu M$, [TEOA] = 10 mM, [DHP] = 8 mM, and $[C_1CP^+] = 230\ \mu M$. Inset: difference spectra revealing the accumulation of C_1CP^0.

creased. Photoreduction of $Co(bpy)_3^{3+}$ required that all reaction components be present; occluded MV^{2+} was also reduced to MV^+ in analogous photoreaction systems when this ion was substituted for $Co(bpy)_3^{3+}$, although these reactions were not studied quantitatively. When internal electron acceptors were omitted, illumination led to accumulation of small amounts of C_1CP^0, as indicated by its characteristic absorption spectrum at 298 nm (Figure 4).[12] In this case, the limiting concentration of accumulated C_1CP^0 observed at long illumination times is not due to exhaustion of any system component but is presumably attributable to accelerating recombination and cross-reactions with other system components in the external medium (see below). No changes in the porphyrin absorption spectra were observed, even following prolonged illumination. This behavior is consistent with the general reaction features outlined in Figure 1, wherein net photoinduced one-electron reduction of C_nCP^+ is followed by transmembrane diffusion of C_nCP^0 and reduction of $Co(bpy)_3^{3+}$ in the internal aqueous phase; the C_nCP^+ ion formed upon reoxidation is trapped within the vesicle. The absence of C_nCP^+ diffusion back into the bulk aqueous phase prevents it from acting cyclically in this system.

Topographic Location of Reaction Components. Partitioning of the reaction components between the membrane−water interface and bulk aqueous phase is expected to strongly influence the photoreaction dynamics of the system.[22,23] The DHP vesicle surfaces are highly negatively charged[23−25] and both strongly electrostatically repel tetraanionic $ZnTPPS^{4-}$ and attract amphiphilic organic cations. For example, binding of alkyl-substituted viologens, for example, *N*-alkyl-*N*′-methyl-4,4′-bipyridinium ions, is extensive and is modulated by the length of the *N*-alkyl chain;[26] for long-chain analogues, hydrophobic forces significantly enhance binding and alter the binding orientation, leading to dramatic changes in reactivity.[3,22−25] Comparable effects can be anticipated for the structurally similar C_nCP^+ ions.

Binding of the C_nCP^+ ions increased progressively with increasing chain length over the range $n = 1-12$. For the $C_{14}CP^+$ and $C_{16}CP^+$ cations, binding was so extensive under all conditions that the concentrations of ions in the bulk aqueous phase were too small to measure. Binding of viologens[27] and other amphiphilic cations[28] to phosphatidylcholine vesicles has been modeled using both Langmuir and Stern adsorption isotherms.[29] In these cases, the quantitative fits obtained did not provide a basis for preferring one model over the other. Consequently, we have chosen herein to use the simpler Langmuir model to describe C_nCP^+ binding to the DHP vesicles. The isotherm is given by

$$p = K(p_{max} - p)[C_nCP^+]_f \quad (1)$$

where K is the apparent binding constant for the C_nCP^+ ions, p is the number of bound C_nCP^+ ions per vesicle under the prevailing conditions, p_{max} is the maximal number of binding sites per vesicle, and $[C_nCP^+]_f$ is the concentration of free C_nCP^+ ions. A typical data fit, for C_8CP^+, is given in Figure 5, for which $K = 1.3 \times 10^3\ M^{-1}$ and $p_{max} = 10^3$. This value of p_{max} corresponds approximately to one C_8CP^+ per 2.6 outer phosphate headgroups of the DHP vesicle.[18] Variations in best-fit values of p_{max} for the different C_nCP^+ ions did not exceed 20% of their average value. Therefore, $p_{max} = 10^3$ was used in all calculations of K for the different cations. The corresponding values of K, summarized in Table 1, indicate that binding increased dramatically with increasing *N*-alkyl chain length. Also shown in Table 1 is the fraction (F) of bound C_nCP^+ ions under conditions approximating those used in the photochemical experiments. This fraction is defined as

$$F = \frac{[C_nCP^+]_b}{[C_nCP^+]_b + [C_nCP^+]_f} \quad (2)$$

where $[C_nCP^+]_b$ is the concentration of bound C_nCP^+ ions. As previously noted, binding of $ZnTPPS^{4-}$ to the vesicles was negligible, although binding of $Co(bpy)_3^{3+}$ was extensive (Table 1).

Oxidative Quenching of $^3ZnTPPS^{4-}$ by C_nCP^+ Ions. Electron transfer from $^3ZnTPPS^{4-}$ to C_1CP^+ is exergonic ($E°(ZnTPPS^{3-}/^3ZnTPPS^{4-}) = -0.75$ V;[16] $E°(C_1CP^+/C_1CP^0) = -0.65$ V[12] in H_2O). For both aqueous solutions and DHP vesicle suspensions, addition of C_nCP^+ ions caused the $^3ZnTPPS^{4-}$ decay rate to increase; transient kinetic spectroscopy revealed simultaneous formation and subsequent decay of the $ZnTPPS^{3-}$ π-cation radical,[30] indicating that oxidative quenching of the photoexcited triplet by C_nCP^+ had occurred. The reaction cycle

$$ZnTPPS^{4-} \xrightarrow{h\nu} {}^3ZnTPPS^{4-} \quad (3)$$

$$^3ZnTPPS^{4-} + C_nCP^+ \xrightarrow{k_q} ZnTPPS^{3-} + C_nCP^0 \quad (4)$$

$$C_nCP^0 + ZnTPPS^{3-} \xrightarrow{k_r} ZnTPPS^{4-} + C_nCP^+ \quad (5)$$

appeared to account quantitatively for the photoresponse, since no changes were detected in the transient absorption spectrum, intermediate decay rate, or ground-state absorption spectrum of the system after exposure to more than 100 laser excitations.

The kinetics of oxidative quenching and charge recombination were complicated by two features. First, addition of C_nCP^+ to $ZnTPPS^{4-}$-containing solutions caused the porphyrin Soret band to red-shift and decrease in intensity. This behavior, which is commonly observed in solutions of water-soluble porphyrins,[22,23,31] is attributable to partial ion-pair complexation of the dye, that is, $ZnTPPS^{4-} + C_nCP^+ \rightleftharpoons (ZnTPPS-C_nCP)^{3-}$. In general, photoexcitation of the ion pair leads to rapid static quenching of the dye excited states. Although this quenching reduces the overall yield of triplets formed in the laser flash, it does not affect the subsequent dynamics of the free reactants. The $^3ZnTPPS^{4-}$ quantum yield was found to decrease progressively with increasing amounts of C_nCP^+ in solution; typical behavior for C_1CP^+ is given in the inset to Figure 6. Assuming 1:1 complexation, one can evaluate from the data an ion-pairing constant of $K_{IP} = 8 \times 10^3\ M^{-1}$, indicating that ~20−60% of

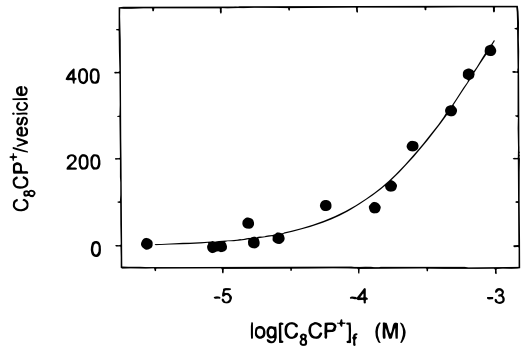

Figure 5. Langmuir adsorption isotherm for C_8CP^+ ion binding to DHP vesicles. Points are data for individual runs, and the solid line is the fit to eq 1 with $p_{max} = 10^3$, $K = 1.3 \times 10^3$ M^{-1}.

TABLE 1: Ion Binding to DHP Vesicles[a]

ion	n	$10^{-3}K$ (M^{-1})[b]	F[c]
C_nCP^+	1	0.016	0.05
	6	1.2	0.70
	8	1.3	0.83
	10	15	0.94
	12	31	0.98
	14	n.d.	~0.99
	16	n.d.	≥0.99
$ZnTPPS^{4-}$		n.d.	<0.05
$Co(bpy)_3^{3+}$		n.d.	0.92

[a] In 20 mM Tris, pH 8.3, at 22 °C with [DHP] = 8 mM. [b] n.d. = not determined. [c] Calculated from eq 2 with 100 μM total C_nCP^+, 12.5 μM total $ZnTPPS^{4-}$, or 28 μM total $Co(bpy)_3^{3+}$.

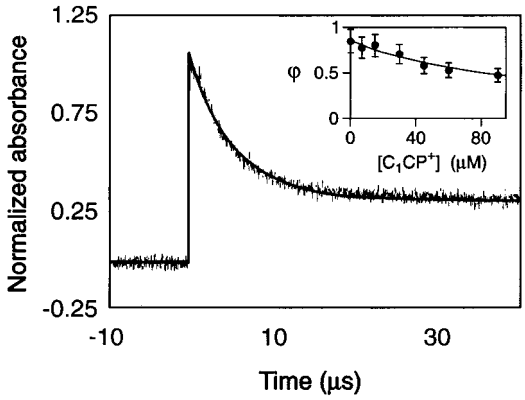

Figure 6. Decay of transient absorption at 460 nm following photoexcitation of $ZnTPPS^{4-}$ in C_1CP^+-containing media: [$ZnTPPS^{4-}$] = 12.5 μM, [C_1CP^+] = 30 μM, [DHP] = 8 mM, laser pulse energy = 23 mJ/pulse. Solid line is theoretical curve calculated according to eq 6 with $A^1_{460} = 1$, $A^2_{460} = 0.3$, $k_q = 5 \times 10^9$ M^{-1} s^{-1}, $\tau = 2.1$ ms, and $k = 540$ s^{-1}. Inset: dependence of the $^3ZnTPPS^{4-}$ quantum yield on the total concentration of C_1CP^+: (●) experimental data; (solid line) data fit assuming a $ZnTPPS^{4-}$−C_1CP^+ ion association constant of $K_{IP} = 8 \times 10^3$ M^{-1}.

the $ZnTPPS^{4-}$ was ion-paired, hence unreactive, under the prevailing reaction conditions. The second complication was that at relatively high laser pulse energies (i.e., $J \geq 100$ mJ/pulse), triplet−triplet annihilation apparently contributed significantly to $^3ZnTPPS^{4-}$ decay.[32−34] This was manifested in nonexponential decay kinetics (which could be fit to a sum of hyperbolic and exponential terms) and the appearance of a rapidly decaying transient in the near-IR region of the spectrum, which could represent formation and decay of porphyrin radical cations and anions formed by ionogenesis,[22,35,36] that is, $2^3ZnTPPS^{4-} \rightarrow ZnTPPS^{3-} + ZnTPPS^{5-} \rightarrow 2ZnTPPS^{4-}$. This potential complication was obviated by conducting the oxidative quenching and charge-recombination kinetic analyses at energies well below 100 mJ/pulse.

Transient kinetic measurements were made at 460 and 650 nm, which correspond to absorption maxima for $^3ZnTPPS^{4-}$ and $ZnTPPS^{3-}$, respectively.[30] The C_nCP^0 radical does not absorb appreciably at $\lambda > 350$ nm; however, at 460 nm, the extinction coefficient of $ZnTPPS^{3-}$ is one-third that of $^3ZnTPPS^{4-}$ so that absorption from both species must be considered in analyzing the absorption decay profiles at this wavelength. At low laser pulse energies, the transient absorption decay kinetics at 460 nm (Figure 6) obeyed the following equation:

$$A_{460}(t) = A^1_{460} \exp(-k_q c_a t - t/\tau) + A^2_{460} \frac{1 - \exp(-k_q c_a t - t/\tau)}{1 + kt} \quad (6)$$

where A^1_{460} and A^2_{460} are constants, c_a is the C_nCP^+ concentration, and τ is the intrinsic $^3ZnTPPS^{4-}$ lifetime, that is, for the reaction

$$^3ZnTPPS^{4-} \xrightarrow{1/\tau} ZnTPPS^{4-} \quad (7)$$

The first term on the right-hand side of eq 6 describes the disappearance of $^3ZnTPPS^{4-}$ by both its intrinsic decay (reaction 7) with the rate constant $1/\tau$ and oxidative quenching by C_nCP^+ (reaction 4) with the rate constant k_q. The second term describes formation and decay of $ZnTPPS^{3-}$ (reactions 4 and 5, respectively); the constant k in the denominator term is proportional to the bimolecular recombination rate constant (k_r) for reaction 5. Equation 6 is valid under the condition that [C_nCP^+] ≫ [$^3ZnTPPS^{4-}$]. The intrinsic triplet lifetime was determined at 460 nm by laser flash excitation of deoxygenated $ZnTPPS^{4-}$ solutions containing no quencher; for both aqueous solutions and DHP vesicle suspensions, $\tau = 2.1$ ms. When C_nCP^+ was present, the absorption decay at 650 nm obeyed the second-order kinetic equation:

$$A_{650}(t) = \frac{A_{650}(0)}{1 + kt} \quad (8)$$

where $A_{650}(0)$ is the maximal absorbance corresponding to formation of $ZnTPPS^{3-}$ and $A_{650}(t)$ is the absorbance at times longer than that required to reach the maximum. As expected for a bimolecular reaction, both $A_{650}(0)$ and k were found to increase linearly with increasing laser pulse energies. The observed rate constant k is related to the bimolecular recombination rate constant k_r through the relationship

$$k_r = \frac{k\epsilon}{A_{650}(0)} \quad (9)$$

where $\epsilon = 8 \times 10^3$ M^{-1} cm^{-1} is the extinction coefficient of $ZnTPPS^{3-}$ at 650 nm.[30] The values of k_r for different *N*-alkylcyanopyridiniums in aqueous solution and vesicular suspensions are given in Table 2. These data were used in eq 6 to determine k_q; a typical plot is given in Figure 6. Best-fit values of the experimental data were obtained with $A^1_{460}/A^2_{460} \simeq 3$, as expected from the relative ϵ values for $^3ZnTPPS^{4-}$ and $ZnTPPS^{3-}$ at this wavelength. Values for k_q determined for different *N*-alkylcyanopyridiniums are given in Table 2.

The values of k_q obtained in homogeneous solution were insensitive to the alkyl chain length, indicating that the inherent reactivities of the different C_nCP^+ ions were nearly identical. In contrast, in the presence of vesicles, k_q decreased progressively with increasing chain length (Table 2). This chain-length dependence correlated with the extent of binding to the vesicles (Table 1), suggesting that the vesicle-bound C_nCP^+ ions were

TABLE 2: Rate Constants for Oxidative Quenching (k_q) and Charge Recombination (k_r)[a]

	H_2O		DHP vesicle suspension	
C_nCP^+ (n)	k_q (M^{-1} s^{-1})	k_r (M^{-1} s^{-1})	k_q (M^{-1} s^{-1})	k_r (M^{-1} s^{-1})
1	4.6×10^9	1.3×10^8	4.7×10^9	8.2×10^7
6	4.4×10^9	1.5×10^8	2.1×10^9	1.3×10^8
8	4.7×10^9	1.0×10^8	5.0×10^8	6.2×10^7
10	4.3×10^9	1.2×10^8	6.7×10^7	3×10^7
12	3.6×10^9	1.4×10^8	1.0×10^7	2.8×10^7
14	n.d.	n.d.	4.5×10^6	2.5×10^7
16	n.d.	n.d.	$<10^6$	1.4×10^8

[a] In 20 mM Tris, pH 8.3, at 22 °C, with [$ZnTPPS^{4-}$] = 12.5 μM, [C_nCP^+] = 12−180 μM, and [DHP] = 8 mM (when present). n.d. = not determined.

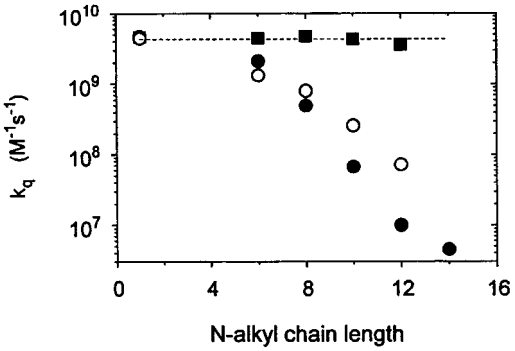

Figure 7. Alkyl chain-length dependence of the quenching rate constants: (●) experimental values of k_q in DHP vesicular suspensions; (○) corresponding k_q values calculated from eq 10 using F values from Table 1 and experimental k_q values for aqueous solutions from Table 2; (■) experimental k_q values for aqueous solutions.

markedly less reactive toward $^3ZnTPPS^{4-}$ than free C_nCP^+. Assuming that the bound quencher is totally unreactive, we obtain using eq 2 an apparent rate constant in vesicular suspensions $(k_q)_v$ given by the expression

$$(k_q)_v = (1 - F)(k_q)_a \qquad (10)$$

where $(k_q)_a$ is the corresponding rate constant in aqueous solution. The experimentally determined rate constants are compared in Figure 7 to $(k_q)_v$ values calculated from eq 10 using data from Tables 1 and 2; the close correspondence observed provides support for the interpretation given.

Two factors might contribute to the absence of reaction between DHP-bound C_nCP^+ ions and $^3ZnTPPS^{4-}$. First, the vesicle interface is highly negatively charged and strongly repels the anionic sensitizer, thereby lowering the reaction rate relative to homogeneous solution. For example, the effective ionic charge of DHP-bound viologen dications has been estimated to be −(10−12) esu from ionic-strength dependencies of reactions with $^3ZnTPPS^{4-}$ and $S_2O_4^{2-}$.[23,25] Second, binding at the DHP vesicle interface is expected to shift the C_nCP^+ reduction potential to more negative values as a consequence of stabilization of the oxidized form through electrostatic interactions with the surfactant phosphate headgroups. Consequently, the reaction driving force would be lowered. Since $\Delta G°$ is small, that is, in the Marcus normal region, the reaction rate should also decrease. For viologen dications, the shift in $E°$ attributable to this effect was as large as −200 mV.[26] This is greater than $\Delta G° = -100$ mV for electron transfer from $^3ZnTPPS^{4-}$ to C_nCP^+ in aqueous solution, suggesting that the analogous reaction involving DHP-bound C_nCP^+ could be thermodynamically uphill by about 100 mV. Charge recombination rate constants (k_r) were also independent of alkyl chain lengths in homogeneous solution (Table 2). Although considerably less sensitive to alkyl chain length than k_q, values of k_r decreased by ∼5-fold for the longest chains when vesicles were present. This reduction in apparent rate constant could arise if some of the product C_nCP^0 formed in the bulk aqueous phase were adsorbed by the vesicles, thereby retarding its recombination reaction with $ZnTPPS^{3-}$. Similar effects have been reported for charge recombination reactions in micelle-containing media.[37]

Reactions with Electron Donors. Standard one-electron reduction potentials for dithiothreitol and its oxidized forms are $E°(DS_2^-, 2H^+/D(SH)_2) = 1.73$ V and $E°(DS_2/DS_2^-) = -1.60$ V.[38] The pK_a for proton dissociation from the disulfide radical is 5.5; consequently, it is anionic under our experimental conditions (pH = 8). It is also highly unstable with respect to disproportionation, that is,

$$2DS_2^- + 2H^+ \rightarrow D(SH_2) + DS_2 \qquad (11)$$

for which $\Delta E = 2.39$ V at pH 8. One-electron reduction of the zinc porphyrin triplet is expected to be energetically unfavorable, that is,

$$^3ZnTPPS^{4-} + D(SH)_2 \rightarrow ZnTPPS^{5-} + DS_2^- + 2H^+ \qquad (12)$$

for which $\Delta E = -0.34$ V (pH 8). Nonetheless, reductive quenching by both $D(SH)_2$ and TEOA were observed. Rate constants, determined from the transient decay kinetics at 460 nm, were 3.2×10^5 M^{-1} s^{-1} for $D(SH)_2$ and -10^4 M^{-1} s^{-1} for TEOA. These values were unchanged when DHP vesicles were included in the reaction medium. The sensitizer absorption spectra and $^3ZnTPPS^{4-}$ quantum yields were unaltered by addition of the donors, suggesting that porphyrin−donor complexes did not form under the experimental conditions. The low rate constants for reductive quenching by $D(SH)_2$ and TEOA undoubtedly reflect the unfavorable energetics of these reactions.

Reduction of $ZnTPPS^{3-}$ produced by oxidative quenching by C_nCP^+ (reaction 4) was accelerated in the presence of the donors. On the basis of reported reduction potentials for $ZnTPPS^{3-}$ ($E°(ZnTPPS^{3-}/ZnTPPS^{4-}) = 0.87$ V)[16] and $D(SH)_2$, the reaction

$$ZnTPPS^{3-} + D(SH)_2 \xrightarrow{k_d} ZnTPPS^{4-} + DS_2^- + 2H^+ \qquad (13)$$

is nearly isoenergetic, that is, $\Delta E = 0.08$ V (pH 8). Bimolecular rate constants, evaluated from the transient decay kinetics at 650 nm, were $\sim 10^6$ M^{-1} s^{-1} for $D(SH)_2$ and 6×10^3 M^{-1} s^{-1} for TEOA. Again, the relatively low rate constants may reflect the relatively small driving force for these electron-transfer steps. Quenching of $^3ZnTPPS^{4-}$ by the donors was negligible under the experimental conditions used for these studies, that is, [$D(SH)_2$] = 0.1−2 mM or [TEOA] = 10−100 mM, [C_nCP^+] = 30−150 μM (with $n \leq 10$), [$ZnTPPS^{4-}$] = 12.5 μM, [DHP] = 8 mM, J = 50−400 mJ/pulse.

Rate Constants for Transmembrane Diffusion of C_nMV^0. Transmembrane diffusion of C_nCP^0 was monitored by measuring the rate of reduction of $Co(bpy)_3^{3+}$ located within the inner aqueous phase of the vesicle following laser pulse generation of C_nCP^0 in the external medium, that is,

$$C_nCP^0 + (Co(bpy)_3^{3+})_i \xrightarrow{k_v} (C_nCP^+ + Co(bpy)_3^{2+})_i \qquad (14)$$

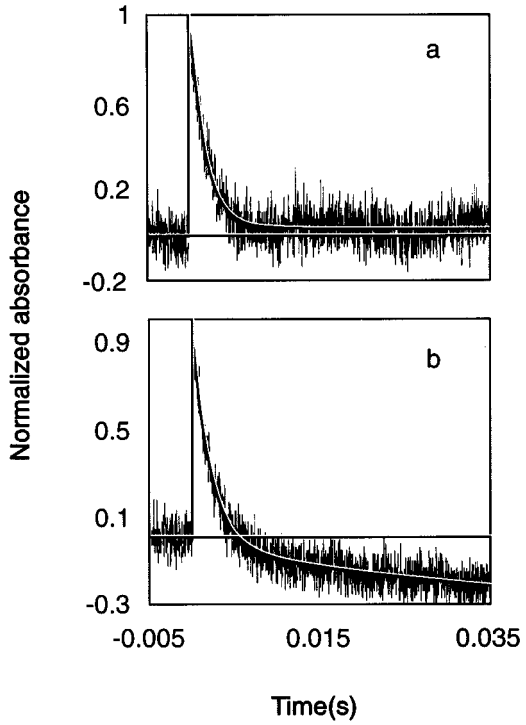

Figure 8. Decay of transient absorption at 313 nm following excitation of the system shown in Figure 1: (a) without occluded $Co(bpy)_3^{3+}$; (b) with $[Co(bpy)_3^{3+}] = 13.5\ \mu M$; $[ZnTPPS^{4-}] = 12.5\ \mu M$; $[C_1CP^+] = 90\ \mu M$; [DHP] = 8 mM; $[D(SH)_2] = 2$ mM; laser pulse energy = 100 mJ/pulse. Solid lines are theoretical curves calculated according to eq 15 with (a) $A_0 = 1$, $\alpha = 0.96$, $\tau_0 = 1.7$ ms, and $A_0^{Co} = 0$ and (b) $A_0 = 1$, $\alpha = 0.96$, $\tau_0 = 1.7$ ms, $A_0^{Co} = -0.3$, and $\tau_v = 25$ ms.

where the notation $(...)_i$ refers to species located within the vesicle. This reaction is expected to be highly exergonic, since $E°(Co(bpy)_3^{3+}/Co(bpy)_3^{2+}) = 0.35$ V, and therefore, $\Delta E° = 1.0$ V for the corresponding reaction in homogeneous solution. To maximize sensitivity, the reaction was monitored at the intense Hg spectral line at 313 nm, which is close to the $Co(bpy)_3^{3+} - Co(bpy)_3^{2+}$ difference spectral minimum (Figure 2). An unknown, fast-decaying transient was detected at this wavelength, which followed exponential decay kinetics, that is, $A(t) = A_0[\alpha \exp(-t/\tau_0) + (1 - \alpha)]$ (Figure 8a). The characteristic decay time of this transient absorption was different for $D(SH)_2$ ($\tau_0 \simeq 1.7$ ms) and TEOA ($\tau_0 \simeq 200\ \mu s$), was observed when $Co(bpy)_3^{3+}$ was absent from the vesicles, and was independent of the concentrations of $ZnTPPS^{4-}$, C_nCP^0, $D(SH)_2$, and TEOA and of the laser pulse energy. No signal was observed when $ZnTPPS^{4-}$ or C_nCP^+ were omitted from the complete reactions system. These properties suggest that transient products of $D(SH)_2$ and TEOA oxidations are the absorbing species.

When $Co(bpy)_3^{3+}$ was included within the vesicles, net bleaching was observed in the transient decay curve monitored at 313 nm (Figure 8b). This reaction was not observed if any of the components of the complete system were omitted (Figure 1). The overall reaction obeyed the following rate law:

$$A(t) = A_0[\alpha \exp(-t/\tau_0) + (1 - \alpha)] + A_0^{Co}[1 - \exp(-t/\tau_v)] \quad (15)$$

where the first term describes the rapidly decaying transient and the second term describes the influence of $Co(bpy)_3^{3+}$ on the kinetic trace. The value of the parameter A_0^{Co} in eq 15 coincides quantitatively with the net photobleaching of the system expected for $Co(bpy)_3^{3+}$ to $Co(bpy)_3^{2+}$ reduction, on the basis of quantum yields calculated from steady-state photolysis experiments (described below). On this basis, we assign the slowly decaying component to transmembrane reduction of $Co(bpy)_3^{3+}$ by C_nCP^+ (reaction 14) which almost certainly occurs by rate-limiting diffusion of the neutral *N*-cyanopyridinium radical. The characteristic relaxation time (τ_v) that gave the best fit to the experimental data was practically the same for all of the *N*-alkylcyanopyridiniums and is equal to 20 ± 7 ms.

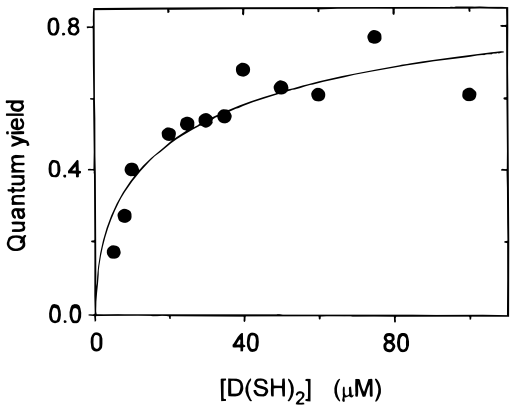

Figure 9. Dependence of quantum yields for $Co(bpy)_3^{3+}$ reduction on the $D(SH)_2$ concentration: $[ZnTPPS^{4-}] = 1\ \mu M$, $[C_1CP^+] = 90\ \mu M$, [DHP] = 8 mM. The solid line is the theoretical fit according to eq 23 with $k_v = 2.3 \times 10^7\ M^{-1}\ s^{-1}$.

Quantum Yields for Transmembrane Reduction. Reaction between C_nCP^+ and $D(SH)_2$, for example,

$$C_1CP^+ + D(SH)_2 \rightarrow C_1CP^0 + DS_2^- + 2H^+ \quad (16)$$

is endergonic ($\Delta E = -1.44$ V at pH 8) and will only occur under these conditions by photosensitized reactions, for example, the sequence of reactions 3, 4, and 13. The reverse reaction is very exergonic, however, and constitutes an energy-dissipating "cross-reaction" in the complete photochemical system, for example, the cycle given by reactions 3, 4, 13, and the reverse of 16. The disulfide radical anion is also capable of reducing C_1CP^+, that is,

$$C_1CP^+ + DS_2^- \xrightarrow{k_{17}} C_1CP^0 + DS_2 \quad (17)$$

for which $\Delta E° = 0.95$ V, so the limiting theoretical quantum yield for C_nCP^0 formation, hence $Co(bpy)_3^{3+}$ reduction, is given by the summation of reactions 16 and 17, that is, $2C_nCP^+ + D(SH)_2 \rightarrow 2C_nCP^0 + DS_2 + 2H^+$. Thus, overall quantum yields as high as $\phi = 2.0$ could be achieved with $D(SH)_2$ as the electron donor, although, in general, the actual value will depend on both the fraction of C_nCP^0 that partitions into the vesicle membrane, thereby escaping charge recombination, and the relative contribution of reaction 17 to the pathways for DS_2^- disappearance, which also include its disproportionation and reactions with C_nCP^0, $^3ZnTPPS^{4-}$, and $ZnTPPS^{3-}$.

Quantum yields for $Co(bpy)_3^{3+}$ reduction to $Co(bpy)_3^{2+}$ measured by continuous photolysis were dependent upon the identity and concentration of C_nCP^+, as well as the $D(SH)_2$ concentration. The dependence upon $D(SH)_2$ concentration is illustrated for C_1CP^+ as the electron carrier in Figure 9; under the experimental conditions, the reaction proceeded exclusively by oxidative quenching. The quantum yields increased at low $D(SH)_2$ but rapidly reached plateau values at $[D(SH)_2] \geq 40\ \mu M$. This behavior is typical of that seen for all the C_nCP^+

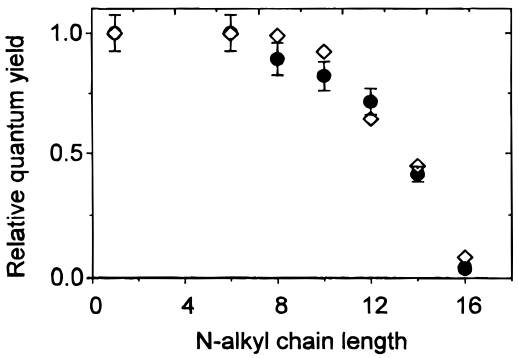

Figure 10. Relative quantum yields for $Co(bpy)_3^{3+}$ reduction mediated by different C_nCP^+ ions: $[ZnTPPS^{4-}] = 1\ \mu M$, $[C_nCP^+] = 90\ \mu M$, $[D(SH)_2] = 100\ \mu M$, [DHP] = 8 mM; (●) experimental data; (◇) relative quantum yields calculated from eq 24 and k_q values from Table 1.

ions, with the exception that the limiting quantum yields decreased with increasing alkyl chain length (Figure 10). As is shown in the following analysis, this dependence reflects the difference in $^3ZnTPPS^{4-}$ quenching rate constants (k_q) for the various C_nCP^+ ions (Table 1).

The data can be analyzed quantitatively by considering reactions 3−5, 7, 13, 14, and 17. Reaction sequences initiated by reductive quenching (reaction 12) are unimportant under the experimental conditions and are not included the reaction scheme. Also excluded are the disproportionation of DS_2^- (reaction 11) and its cross-reactions with C_nCP^0 (reverse of 16), $^3ZnTPPS^{4-}$, and $ZnTPPS^{3-}$. Each of these involves bimolecular reactions in which the steady-state concentration of the second reactant is vanishingly small. Assuming that each C_nCP^0 that is captured by a vesicle diffuses across its membrane to reduce $Co(bpy)_3^{3+}$, the rate law for transmembrane reduction is given by

$$-\frac{d[Co(bpy)_3^{3+}]}{dt} = k_v[C_nCP^0]c_v = \phi_n I_a \qquad (18)$$

where c_v is the concentration of vesicles and I_a is the number of photons absorbed by $ZnTPPS^{4-}$ in einstein L^{-1} s^{-1}. The steady-state conditions for $^3ZnTPPS^{4-}$, $ZnTPPS^{3-}$, C_nCP^0, and DS_2^- are given by the following equations:

$$\frac{d[^3ZnTPPS^{4-}]}{dt} = \varphi I_a - \frac{1}{\tau}[^3ZnTPPS^{4-}] - k_q[^3ZnTPPS^{4-}]c_a = 0 \quad (19)$$

$$\frac{d[C_nCP^0]}{dt} = k_q[^3ZnTPPS^{4-}]c_a + k_{17}[DS_2^-]c_a - k_r[C_nCP^0][ZnTPPS^{3-}] - k_v[C_nCP^0]c_v = 0 \quad (20)$$

$$\frac{d[ZnTPPS^{3-}]}{dt} = k_q[^3ZnTPPS^{4-}]c_a - k_r[C_nCP^0][ZnTPPS^{3-}] - k_d[ZnTPPS^{3-}]c_d = 0 \quad (21)$$

$$\frac{d[DS_2^-]}{dt} = k_d[ZnTPPS^{3-}]c_d - k_{17}[DS_2^-]c_a = 0 \quad (22)$$

In these equations, φ is the quantum yield for $^3ZnTPPS^{4-}$ formation and c_d is the concentration of $D(SH)_2$. Combining eqs 18−22, one obtains

$$\phi = \frac{\sqrt{(k_d k_v c_d c_v - 2k_r k_d c_T c_d)^2 + 8k_q k_r k_d k_v c_a c_T c_d c_v}}{2k_r I_a} - \frac{(k_d k_v c_d c_v - 2k_r k_d c_T c_d)}{2k_r I_a} \qquad (23)$$

where

$$c_T = \frac{\varphi I_a \tau}{1 + \tau k_q c_a}$$

is the steady-state concentration of the excited triplet molecules.

At $D(SH)_2$ concentrations that are sufficiently large that reaction 13 predominates over reaction 5, that is, where nearly every $ZnTPPS^{3-}$ formed generates a DS_2^- radical, eq 23 reduces to

$$\phi = \frac{2\varphi\tau k_q c_a}{1 + \tau k_q c_a}$$

The relative quantum yields for $Co(bpy)_3^{3+}$ reduction obtained in this limit are therefore given by

$$\frac{(\phi)_n}{(\phi)_1} = \frac{(k_q)_n(1 + \tau(k_q)_1 c_a)}{(k_q)_1(1 + \tau(k_q)_n c_a)} \qquad (24)$$

where the subscript n is used to identify specific C_nCP^+ ions being compared.

Values calculated for different C_nCP^+ relative to C_1CP^+ are nearly identical to experimentally determined values (Figure 10), consistent with the assumptions implicit in the reaction scheme.

The rate constant (k_v) for C_1CP^0 capture by the DHP vesicles can be evaluated from eq 23 using the experimentally determined values for ϕ_1, φ, k_q, k_r, and k_d. The value that gave the best fit to the data (Figure 9) is $k_v = 2.3 \times 10^7\ M^{-1}\ s^{-1}$. This value is very similar to one that can be estimated from the value of τ_v measured by flash photolysis (Figure 8b). Assuming that $k_v = (\tau_v c_v)^{-1}$, we obtain $k_v = 2.5 \times 10^7\ M^{-1}\ s^{-1}$ when $c_v = 2\ \mu M$ (Figure 8). This rate constant is more than 3 orders of magnitude less than the bimolecular rate constant for diffusion-controlled reactions involving DHP vesicles ($k_D \approx 10^{11}\ M^{-1}\ s^{-1}$), indicating that transmembrane diffusion of C_nCP^0 is the rate-limiting step. The characteristic time for transmembrane diffusion ($\tau_v = 2 \times 10^{-2}$ s) is about 2 orders of magnitude more than characteristic times of transmembrane diffusion of neutral lipophilic ions such as protonophores across the phospholipid bilayer membranes ($\tau_v \approx 10^{-4}$ s).[39,40] This difference may be due to the lower fluidity of the DHP membrane, which is in its ordered, or gel, phase,[18] in comparison to the liposome, which is in its liquid crystalline phase. The transmembrane diffusion coefficient of C_nCP^0, estimated from the Smoluchowski−Einstein equation, $D \approx l^2/\tau_v$, where $l \approx 4$ nm is the hydrocarbon bilayer width, is approximately $10^{-11}\ cm^2\ s^{-1}$. This corresponds to a permeability coefficient $P = l/\tau_v \approx 2 \times 10^{-5}$ cm/s.

Acknowledgment. The authors thank Alexsander Noy for preliminary experiments establishing the feasibility of these studies and Peter Brezny for synthesizing some of the *N*-alkyl-4-cyanopyridinium compounds. Funding for this research was provided by the Division of Chemical Sciences, Office of Basic Energy Sciences, U.S. Department of Energy under Grant DE-FG06-95ER14581.

References and Notes

(1) Harold, F. M. *The Vital Force: A Study in Bioenergetics*; Freeman: New York, 1986.

(2) Nicholls, D. G.; Ferguson, S. J. *Bioenergetics 2*; Academic Press: New York, 1992.
(3) Hurst, J. K. In *Kinetics and Catalysis in Microheterogeneous Systems*; Gratzel, M., Kalyanasundaram, K., Eds.; Surfactant Science Series 38; Marcel Dekker: New York, 1991; p 183.
(4) Lymar, S. V.; Parmon, V. N.; Zamaraev, K. I. In *Photoinduced Electron Transfer III*; Mattay, J., Ed.; Topics in Current Chemistry 159; Springer-Verlag: Berlin, 1991; p 1.
(5) Alfimov, M. V.; Khairutdinov, R. F. *Usp. Nauchn. Fotogr.* **1989**, *25*, 154.
(6) Steinberg-Yfrach, G.; Liddell, P. A.; Hung, S.-C.; Moore, A. L.; Gust, D.; Moore, T. A. *Nature* **1997**, *385*, 239.
(7) Hammarstrom, L.; Almgren, M.; Norrby, T. *J. Phys. Chem.* **1992**, *96*, 5017.
(8) Patterson, B. C.; Hurst, J. K. *J. Phys. Chem.* **1993**, *97*, 454.
(9) Kuhn, E. R.; Hurst, J. K. *J. Phys. Chem.* **1993**, *97*, 1712.
(10) Lymar, S. V.; Hurst, J. K. *J. Phys. Chem.* **1994**, *98*, 989.
(11) Lymar, S. V.; Hurst, J. K. *J. Am. Chem. Soc.* **1992**, *114*, 9498.
(12) Harriman, A.; Millward, G. R.; Neta, P.; Richoux, M. C.; Thomas, J. M. *J. Phys. Chem.* **1988**, *92*, 1286.
(13) Hermolin, J.; Levin, M.; Ikegami, Y.; Sawayanagi, M.; Kosower, E. M. *J. Am. Chem. Soc.* **1981**, *103*, 4795.
(14) Kitamura, N.; Nambu, Y.; Endo, T. *J. Polym. Sci. A* **1990**, *28*, 3137.
(15) Kosower, E. M.; Cotter, J. L. *J. Am. Chem. Soc.* **1964**, *86*, 5524.
(16) Kalyanasundaram, K.; Neumann-Spallart, M. *J. Phys. Chem.* **1982**, *86*, 5163.
(17) Burstall, F. H.; Nyholm, R. S. *J. Chem. Soc.* **1952**, 3570.
(18) Humphry-Baker, R.; Thompson, D. H.; Lei, Y.; Hope, M. J.; Hurst, J. K. *Langmuir* **1991**, *7*, 2592.
(19) Hatchard, C. G.; Parker, C. A. *Proc. R. Soc., Ser. A* **1956**, *235*, 518.
(20) Wegner, E. E.; Adamson, A. W. *J. Am. Chem. Soc.* **1966**, *88*, 394.
(21) Lessard, J. G.; Fragata, M. *J. Phys. Chem.* **1986**, *90*, 811.
(22) Hurst, J. K.; Lee, L. Y. C.; Gratzel, M. *J. Am. Chem. Soc.* **1983**, *105*, 7048.
(23) Hurst, J. K.; Thompson, D. H. P.; Connolly, J. S. *J. Am. Chem. Soc.* **1987**, *109*, 507.
(24) Hurst, J. K.; Thompson, D. H. P. *Inorg. Chem.* **1987**, *26*, 39.
(25) Thompson, D. H. P.; Barrette, W. C., Jr.; Hurst, J. K. *J. Am. Chem. Soc.* **1987**, *109*, 2003.
(26) Lei, Y.; Hurst, J. K. *J. Phys. Chem.* **1991**, *95*, 7918.
(27) Lee, L. Y. C. Ph.D. Dissertation, Oregon Graduate Center, 1985.
(28) Kuhn, E. R. Ph.D. Dissertation, Oregon Graduate Institute of Science & Technology, 1989.
(29) McLaughlin, S. *Curr. Top. Membr. Transp.* **1977**, *9*, 71.
(30) Neta, P. *J. Phys. Chem.* **1981**, *85*, 3678.
(31) Rougee, M.; Ebbeson, T.; Ghetti, F.; Bensasoon, R. V. *J. Phys. Chem.* **1982**, *86*, 4404.
(32) Linschitz, H.; Sarkanen, K. *J. Am. Chem. Soc.* **1958**, *80*, 4826.
(33) Pekkarinen, L.; Linschitz, H. *J. Am. Chem. Soc.* **1960**, *82*, 2407.
(34) Houlding, V. H.; Kalyanasundaram, K.; Gratzel, M.; Milgrom, L. R. *J. Phys. Chem.* **1983**, *87*, 3175.
(35) Ballard, S. G.; Mauzerall, D. C. *J. Chem. Phys.* **1980**, *72*, 933.
(36) Carapellucci, P. A.; Mauzerall, D. *Ann. N.Y. Acad. Sci.* **1975**, *244*, 214.
(37) Brugger, P.-A.; Infelta, P. P.; Braun, A. M.; Gratzel, M. *J. Am. Chem. Soc.* **1981**, *103*, 320.
(38) Surdhar, P. S.; Armstrong, D. A. *J. Phys. Chem.* **1987**, *91*, 6532.
(39) Bradshaw, R. W.; Robertson, C. R. *J. Membr. Biol.* **1975**, *25*, 93.
(40) Kasianowicz, J.; Benz, R.; McLaughlin, S. *J. Membr. Biol.* **1984**, *82*, 179.